

UNCLASSIFIED

AD NUMBER
AD491094
NEW LIMITATION CHANGE
TO Approved for public release, distribution unlimited
FROM Distribution authorized to U.S. Gov't. agencies and their contractors; Administrative/Operational Use; AUG 1960. Other requests shall be referred to David Taylor Model Basin, Washington, DC.
AUTHORITY
DTMB ltr, 28 Dec 1965

THIS PAGE IS UNCLASSIFIED

UNCLASSIFIED

AD **491094**

DEFENSE DOCUMENTATION CENTER

FOR

SCIENTIFIC AND TECHNICAL INFORMATION

CAMERON STATION ALEXANDRIA, VIRGINIA



UNCLASSIFIED

NOTICE: When government or other drawings, specifications or other data are used for any purpose other than in connection with a definitely related government procurement operation, the U. S. Government thereby incurs no responsibility, nor any obligation whatsoever; and the fact that the Government may have formulated, furnished, or in any way supplied the said drawings, specifications, or other data is not to be regarded by implication or otherwise as in any manner licensing the holder or any other person or corporation, or conveying any rights or permission to manufacture, use or sell any patented invention that may in any way be related thereto.

UNANNOUNCED

Report 1392



DEPARTMENT OF THE NAVY
DAVID TAYLOR MODEL BASIN

CATALOGED BY DDC

HYDROMECHANICS

AERODYNAMICS

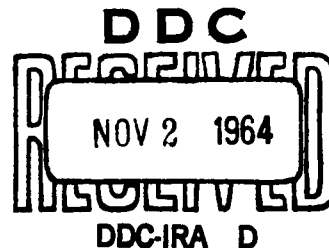
STRUCTURAL
MECHANICS

APPLIED
MATHEMATICS

INELASTIC LOBAR BUCKLING OF CYLINDRICAL SHELLS
UNDER EXTERNAL HYDROSTATIC PRESSURE

by

Thomas E. Reynolds



STRUCTURAL MECHANICS LABORATORY
RESEARCH AND DEVELOPMENT REPORT

August 1960

Report 1392

**INELASTIC LOBAR BUCKLING OF CYLINDRICAL SHELLS
UNDER EXTERNAL HYDROSTATIC PRESSURE**

by

Thomas E. Reynolds

August 1960

**Report 1392
S-F013 03 02**

TABLE OF CONTENTS

	Page
ABSTRACT.....	1
INTRODUCTION	1
ANALYSIS.....	2
Plastic Buckling Equations	2
Elastic Buckling Equations	5
Minimization of Expressions for Buckling Pressure.....	6
Determination of Secant and Tangent Moduli.....	9
Inelastic Buckling	13
EVALUATION OF THEORY WITH EXPERIMENTAL DATA ON STIFFENED CYLINDERS	15
CONCLUSIONS.....	20
ACKNOWLEDGMENTS	20
APPENDIX – DERIVATION OF BUCKLING EQUATIONS.....	21
REFERENCES	25

LIST OF FIGURES

Figure 1 – Buckling-Mode Parameter ϕ as a Function of \sqrt{Rt}/L	8
Figure 2 – Comparison of Approximate and Exact Methods for Determining Minimum Buckling Pressure	10
Figure 3 – Typical Stress-Strain Diagram	11
Figure 4 – Graphical Determination of Buckling Pressure for Two General Classes of Material.....	16
Figure 5 – Compression Curves for Cylinder Materials.....	18
Figure 6 – Comparison of Theoretical and Experimental Collapse Pressures.....	19
Figure 7 – Coordinate System and Cross Section of Stiffened Shell.....	22

LIST OF TABLES

Table 1 – Properties of Cylinders	17
Table 2 – Comparison of Theoretical and Experimental Collapse Pressures.....	17

NOTATION

A	Arbitrary constant
A_i	Plasticity coefficients
A_f	Area of cross section of ring
a	Small dimensionless quantity
b	Faying width of frame
c	$(E_s/E_t) - 1$
D	Bending rigidity, $E_s h^3/12 (1 - \nu^2)$
E	Young's modulus
E_s	Secant modulus
E_t	Tangent modulus
F	$(E_t/E_s) \left(\frac{1}{2} \frac{\partial u}{\partial x} + \frac{\partial v}{\partial s} + \frac{w}{R} \right)$
f	Stress ratio, σ_x/σ_s
h	Shell thickness
k	n/R
L	Unsupported length of cylinder
m, n	Integers
N	$(\cosh \theta - \cos \theta)/(\sinh \theta + \sin \theta)$
N_s, N_x, N_{xs}	Forces per unit length
p	Pressure
p_e	Elastic buckling pressure
p_c	Inelastic buckling pressure
p_p	Plastic buckling pressure
R	Radius of cylinder
s	Circumferential coordinate
u, v, w	Shell displacements

s	Axial coordinate
α	$(3/\sigma_i^2) (1 - E_i/E_s)$
β	$\theta (\sinh \theta + \sin \theta)/(\cosh \theta - \cos \theta)$
β'	$\frac{\theta}{2} \left(\sinh \frac{\theta}{2} + \sin \frac{\theta}{2} \right) / \left(\cosh \frac{\theta}{2} - \cos \frac{\theta}{2} \right)$
γ	Shear strain
ϵ_s, ϵ_x	Membrane strains
ϵ_i	Strain intensity
θ	$(L/\sqrt{Rh}) [3(1 - \gamma^2)]^{1/4}$
λ	$m\pi/L$
ν	Poisson's ratio
ν_e	Elastic value of Poisson's ratio
$\sigma_s; \sigma_x = \frac{pR}{2h}$	Circumferential and axial stresses
σ_i	Stress intensity
ϕ	$\lambda^2/(\lambda^2 + k^2)$
∇^4	Operator, $\left[\frac{\partial^2}{\partial x^2} + \frac{\partial^2}{\partial s^2} \right]^2$
∇^8	$(\nabla^4)^2$

ABSTRACT

A solution to Gerard's differential equations for plastic buckling of cylindrical shells is found for the case of lobar buckling under hydrostatic pressure. An approximate formula based on this solution is then obtained for buckling in the inelastic region.

According to this formula, the buckling pressure is a function of the cylinder geometry and the secant and tangent moduli as determined from a stress-strain intensity diagram for the shell material. Agreement with experiments on ring-stiffened cylinders is found to be within 4 percent.

INTRODUCTION

Experimental studies of the buckling of stiffened cylinders under hydrostatic pressure have shown that collapse of the shell plating between frames is frequently preceded by yielding of the shell material. This would indicate that inelastic shell buckling may be an important consideration in the strength design of pressure vessels, particularly when it is realized that residual welding and rolling stresses often induce inelastic behavior at pressures well below the design strength.

Inelastic buckling of cylindrical shells induced by external hydrostatic pressure can take place in two basic modes: axisymmetric buckling, during which circumferential corrugations develop along the axis, and asymmetric or lobar buckling, whereby inward and outward lobes appear alternately around the circumference. Buckling of the first type has received considerable attention, but it has usually been treated as a failure due to yielding rather than a buckling phenomenon. Typically, an analysis is based on the concept of an ideal material which, at a certain stress level, undergoes an abrupt transition to the perfectly plastic state. The buckling pressure is determined not from stability considerations but from the state-of-equilibrium stresses. Attempts to describe buckling of the second type have been rather limited and have usually depended on the intuitive use of a reduced modulus in place of Young's modulus in the elastic buckling equation.

In recent years, however, advances in plasticity theory have made it possible to approach these problems more rigorously. Investigations by Bijlaard,^{1,2} Ilyushin,³ and Stowell,⁴ among others, have contributed greatly to the development of theory for the inelastic buckling of plates and shells. More recently, Gerard⁵ derived a general set of differential equations for cylinders from which he obtained approximate solutions for torsional buckling and axisymmetric buckling under axial compression for a strain-hardening material. Lunchick⁶ has since developed a similar, but more exact, theory for axisymmetric buckling

¹References are listed on page 25.

of ring-stiffened cylinders under hydrostatic pressure. From recent tests conducted at the David Taylor Model Basin, this theory appears to be very reliable.

At the same time, it appeared that the work of Gerard might also provide a worthwhile approach to the problem of asymmetric or lobar buckling in ring-stiffened cylinders, since his differential equations are sufficiently general to account for asymmetric deformations under hydrostatic loading. Work was subsequently initiated to obtain a solution to Gerard's equations for the asymmetric problem. In this report the solution is derived, and an approximate formula for inelastic buckling is obtained. Experimental data from ring-stiffened cylinders are used to evaluate the formula.

ANALYSIS

PLASTIC BUCKLING EQUATIONS

In the Appendix of this report, the general differential equations of Gerard⁵ for a fully plastic cylinder are specialized for the case of hydrostatic pressure loading. The buckling equations thereby obtained are:

$$\frac{E_t}{2E_s} \left(\frac{1}{2} \frac{\partial^2 u}{\partial x^2} + \frac{\partial^2 v}{\partial x \partial s} + \frac{1}{R} \frac{\partial w}{\partial x} \right) + \frac{3}{4} \frac{\partial^2 u}{\partial x^2} + \frac{1}{4} \frac{\partial^2 u}{\partial s^2} + \frac{1}{4} \frac{\partial^2 v}{\partial x \partial s} = 0 \quad [1a]$$

$$\frac{E_t}{E_s} \left(\frac{1}{2} \frac{\partial^2 u}{\partial x \partial s} + \frac{\partial^2 v}{\partial s^2} + \frac{1}{R} \frac{\partial w}{\partial s} \right) + \frac{1}{4} \frac{\partial^2 v}{\partial x^2} + \frac{1}{4} \frac{\partial^2 u}{\partial x \partial s} = 0 \quad [1b]$$

$$\begin{aligned} \frac{4E_s h}{3R} \left(\frac{E_t}{E_s} \right) \left(\frac{1}{2} \frac{\partial u}{\partial x} + \frac{\partial v}{\partial s} + \frac{w}{R} \right) + D \left[\frac{E_t}{E_s} \left(\frac{1}{4} \frac{\partial^4 w}{\partial x^4} + \frac{\partial^4 w}{\partial x^2 \partial s^2} + \frac{\partial^4 w}{\partial s^4} \right) + \frac{3}{4} \frac{\partial^4 w}{\partial x^4} + \frac{\partial^4 w}{\partial x^2 \partial s^2} \right] \\ + N_x \frac{\partial^2 w}{\partial x^2} + N_s \frac{\partial^2 w}{\partial s^2} + p = 0 \end{aligned} \quad [1c]$$

where x and s are respectively the axial and circumferential coordinates,
 u , v , and w are the axial, tangential, and radial displacements,
 E_s and E_t are the secant and tangent moduli,
 R is the radius to the shell midsurface,
 h is the shell thickness,
 ν is Poisson's ratio,

D is the bending rigidity $= E_s h^3 / 12(1 - \nu^2)$,

N_x and N_s are forces per unit length in the axial and circumferential directions, and

p is the hydrostatic pressure.

Since one function recurs in all three equations, let

$$F = \frac{E_t}{E_s} \left(\frac{1}{2} \frac{\partial u}{\partial x} + \frac{\partial v}{\partial s} + \frac{w}{R} \right) \quad [2]$$

With several differentiations, u and v can be eliminated from Equations [1a] and [1b] so that one equation relating F and w results:

$$\frac{E_t}{E_s} \left(\frac{\partial^4 F}{\partial x^4} + 8 \frac{\partial^4 F}{\partial x^2 \partial s^2} + 4 \frac{\partial^4 F}{\partial s^4} \right) + 3 \frac{\partial^4 F}{\partial x^4} = \frac{3}{R} \frac{E_t}{E_s} \frac{\partial^4 w}{\partial x^4} \quad [3]$$

With suitable differentiations, Equation [1c] can be combined with Equation [3] so that a single eight-order equation in w is obtained:

$$\begin{aligned} D \left\{ \frac{E_t}{E_s} \nabla^8 w + \left(1 - \frac{E_t}{E_s} \right) \left[\nabla^4 \left(\frac{3}{2} \frac{\partial^4 w}{\partial x^4} + \frac{\partial^4 w}{\partial x^2 \partial s^2} \right) + \frac{3}{4} \left(\frac{E_s}{E_t} - 1 \right) \left(\frac{3}{4} \frac{\partial^8 w}{\partial x^8} + \frac{\partial^8 w}{\partial x^6 \partial s^2} \right) \right] \right\} \\ + \frac{E_s h}{R^2} \frac{\partial^4 w}{\partial x^4} + N_x \left[\nabla^4 \frac{\partial^2 w}{\partial x^2} + \frac{3}{4} \left(\frac{E_s}{E_t} - 1 \right) \frac{\partial^6 w}{\partial x^6} \right] \\ + N_s \left[\nabla^4 \frac{\partial^2 w}{\partial s^2} + \frac{3}{4} \left(\frac{E_s}{E_t} - 1 \right) \frac{\partial^6 w}{\partial x^4 \partial s^2} \right] = 0 \end{aligned} \quad [4]$$

where ∇^4 indicates the operator $\left[\frac{\partial^2}{\partial x^2} + \frac{\partial^2}{\partial s^2} \right]^2$

A solution to this equation can be written:

$$w = A \sin ks \sin \lambda x \quad [5]$$

$$\text{where } k = \frac{n}{R}$$

$$\lambda = \frac{m\pi}{L}$$

L is the length of the shell, and

m and n are integers.

This solution satisfies the conditions of simple support at the ends of the cylinder; i.e., that w and $\frac{\partial^2 w}{\partial x^2}$ vanish at $x = 0$ and $x = L$. These conditions are not unreasonable for stiffened cylinders since it is likely that the effective rotational restraint will be limited by the formation of plastic regions arising from high bending stresses near stiffeners or end supports.

By substituting the solution [5] into the differential Equation [4], the following characteristic-value equation is obtained:

$$D \left\{ \frac{E_t}{E_s} (k^2 + \lambda^2)^4 + \left(1 - \frac{E_t}{E_s} \right) \lambda^2 \left[(k^2 + \lambda^2)^2 \left(\frac{3\lambda^2}{2} + k^2 \right) + \frac{3\lambda^4}{4} \left(\frac{E_s}{E_t} - 1 \right) \left(\frac{3\lambda^2}{4} + k^2 \right) \right] \right\} \\ + \frac{E_s h}{R^2} \lambda^4 - \frac{pR}{2} \left\{ (k^2 + \lambda^2)^2 \lambda^2 + \frac{3}{4} \left(\frac{E_s}{E_t} - 1 \right) \lambda^6 + \frac{2N_s}{pR} \lambda^2 \left[(k^2 + \lambda^2)^2 \right. \right. \\ \left. \left. + \frac{3}{4} \left(\frac{E_s}{E_t} - 1 \right) \lambda^4 \right] \right\} = 0 \quad [6]$$

To simplify this equation the following substitutions are made:

$$\phi = \frac{\lambda^2}{\lambda^2 + k^2} = \frac{1}{\left(1 + \frac{n^2 L^2}{m^2 \pi^2 R^2} \right)}$$

$$f_p = \frac{pR}{2N_s} = \frac{\sigma_x}{\sigma_s} \quad [7]$$

$$C = \left(\frac{E_s}{E_t} \right) - 1$$

The equation is then rearranged so that an expression for p_p , the plastic buckling pressure, is obtained:

$$p_p = \frac{2f_p D \lambda^2 \frac{E_t}{E_s} \left\{ 1 + C \phi \left[1 + \frac{\phi}{2} + 3 \frac{C \phi^2}{4} \left(1 - \frac{\phi}{4} \right) \right] \right\} + 2 \frac{E_s h f_p \phi^4}{R^2 \lambda^2}}{R \phi [1 - \phi (1 - f_p)] \left[1 + 3 \frac{C \phi^2}{4} \right]} \quad [8]$$

*The subscript on f indicates the stress ratio for the plastic region.

ELASTIC BUCKLING EQUATIONS

A similar procedure is followed in obtaining a solution for the elastic case. When $\frac{E_t}{E_s}$ is set equal to unity, Equation [4] reduces to

$$D \nabla^8 w + \frac{Eh}{R^2} \frac{\partial^4 w}{\partial x^4} + \nabla^4 \left(N_x \frac{\partial^2 w}{\partial x^2} + N_s \frac{\partial^2 w}{\partial s^2} \right) = 0 \quad [9]$$

which is the Donnell equation^{5,7} for the case of hydrostatic pressure loading. The bending rigidity is now given by

$$D = \frac{Eh^3}{12(1-\nu_e^2)} \quad [10]$$

where ν_e is the elastic value of Poisson's ratio. Substitution of solution [5] into Equation [9] yields*

$$p_e = 2f_e \frac{Eh}{R\phi} \left[\frac{\frac{h^2\lambda^2}{12(1-\nu_e^2)} + \frac{\phi^4}{R^2\lambda^2}}{1-\phi(1-f_e)} \right] \quad [11]$$

where f_e is the stress ratio for the elastic region. This equation could have been obtained directly from Equation [8] by using the elastic value for D .

*It is of some interest to compare this result with a similar equation obtained by Von Sanden and Tölke⁸ in their comprehensive study of stability problems in thin cylindrical shells. In considering the elastic buckling of a ring-stiffened cylinder, they allow for the variability of the pre-buckling circumferential stress with the axial coordinate. Their buckling pressure equation, in the terminology of this report is:

$$p_e = \frac{2Eh}{R\phi} \left[\frac{\frac{h^2\lambda^2}{12(1-\nu_e^2)} + \frac{\phi^4}{R^2\lambda^2}}{\frac{\phi}{2} + (1-\phi) \left(\frac{3\delta_m}{4} + \frac{\delta_0}{4} \right)} \right]$$

where $(\sigma_s)_{x=\frac{L}{2}} = \delta_m \frac{pR}{h}$ = midbay circumferential stress

$(\sigma_s)_{x=0} = \delta_0 \frac{pR}{h}$ = circumferential stress at a frame

and δ_m and δ_0 are determined from the theory of Von Sanden and Gunther.⁹

If σ_s does not vary with x , then

$$\delta_m = \delta_0 = \delta = \frac{1}{2f_e}$$

and the buckling pressure equation reduces to Equation [11].

MINIMIZATION OF EXPRESSIONS FOR BUCKLING PRESSURE

Equation [8] expresses p_p , the plastic buckling pressure, in terms of n , the number of circumferential buckling waves, and m , the number of longitudinal half waves. The buckling pressure can now be obtained in minimized form. It can be seen that p_p is effectively minimized with respect to n/m by setting

$$\frac{\partial p_p}{\partial \phi} = 0 \quad [12]$$

The resulting equation defines the value of ϕ_p for which p_p is a minimum:

$$\phi_p^4 = \frac{m^4 \pi^4}{9} \frac{E_t}{E_s} \left(\frac{\sqrt{R}h}{L} \right)^4 \left[\frac{1 - 2\phi_p (1 - f_p) + \frac{3C\phi_p^2}{4}}{3 - 2\phi_p (1 - f_p) + \frac{3C\phi_p^2}{4}} \right] \times \left\{ 1 + \frac{\frac{3C\phi_p^2}{4} \left[\frac{4f_p}{3} - 4\phi_p (1 - f_p) + \frac{C\phi_p^2}{4} |8f_p - 3 - 6\phi_p^2 (1 - f_p)| \right]}{1 - 2\phi_p (1 - f_p) + \frac{3C\phi_p^2}{4}} \right\} \quad [13]$$

The corresponding equation for the minimized plastic buckling pressure is:

$$p_p = \frac{8m^2 \pi^2 E_t f_p}{9\phi_p} \left(\frac{h}{R} \right)^2 \left(\frac{\sqrt{R}h}{L} \right)^2 \left[\frac{1 + \frac{C\phi_p}{4} \left(3 + \phi_p + \frac{3C\phi_p^2}{4} \right)}{3 - 2\phi_p (1 - f_p) + \frac{3C\phi_p^2}{4}} \right] \quad [14]$$

which is obtained through suitable combination of Equations [8] and [13]. Since p_p in Equation [4] is proportional to m^2 , it is clear that for the minimum value of p_p m must be equal to one in all cases where n is greater than 0.

The corresponding minimized equations can be obtained for the elastic case. After minimizing p_e with respect to ϕ in Equation [11], one obtains the equivalents of Equations [13] and [14] for the elastic case:

$$\phi_e^4 = \frac{\pi^4 m^4}{12(1 - \nu_e^2)} \left(\frac{\sqrt{R}h}{L} \right)^4 \left[\frac{1 - 2\phi_e (1 - f_e)}{3 - 2\phi_e (1 - f_e)} \right] \quad [15]$$

$$p_e = \frac{2\pi^2 m^2 E f_e}{3(1-\nu_e^2)\phi_e} \left(\frac{h}{R}\right)^2 \left(\frac{\sqrt{Rh}}{L}\right)^2 \left[\frac{1}{3-2\phi_e(1-f_e)} \right] \quad [16]$$

These equations could also have been obtained directly from Equations [13] and [14]. Again it is seen that m must be equal to 1. For the case where f_e is equal to $\frac{1}{2}$ corresponding to the prebuckling state of stress in an unstiffened tube, it can be shown that Equations [15] and [16] are exactly those given by Windenburg and Trilling (Equations [20] and [21] of Reference 10) in expressing the Von Mises buckling pressure in minimized form.

Although Equations [14] and [16] are relatively simple in form, they contain the function ϕ which is not readily determinable from Equations [13] and [15]. However, it is possible to obtain an approximate expression for ϕ from a graphical representation of these equations. Figure 1 shows plots of ϕ versus \sqrt{Rh}/L (with m equal to one) for the following cases:

$$\begin{aligned} \text{Elastic: } \frac{E_t}{E_s} &= 1 \quad \nu_e = 0.3 \quad \left\{ \begin{array}{l} f_e = \frac{1}{2} \\ f_e = 1 \end{array} \right. \\ \text{Plastic: } \frac{E_t}{E_s} &= \frac{1}{2} \quad \nu = \frac{1}{2} \quad \left\{ \begin{array}{l} f_p = \frac{1}{2} \\ f_p = 1 \end{array} \right. \end{aligned}$$

The value of $\frac{1}{2}$ for E_t/E_s was chosen as a typical case for the plastic region. The two stress ratios, $\frac{1}{2}$ and 1, are extreme values which should bound all cases of practical interest. The curves terminate at the line where ϕ is equal to 1, since this is the case of axisymmetric ($n = 0$) buckling for which the minimized pressure expressions no longer have meaning. These curves suggest that a simple linear relationship between ϕ and \sqrt{Rh}/L might serve as an adequate approximation for all cases. Use of such an approximation implies that the number of circumferential lobes is independent of the material properties. After some investigation, the equation

$$\phi = 1.23 \frac{\sqrt{Rh}}{L} \quad [17]$$

represented by the dotted line in Figure 1, was chosen as a reasonably good approximation.* It is seen that this line falls roughly midway between the extremes of the curves presented. Use of Equation [17] in conjunction with Equations [14] and [16] then provides approximate expressions for p_p and p_e . It is also helpful to make an additional approximation which

*Actually, the selection of the factor 1.23 was somewhat arbitrary since the buckling pressure is relatively insensitive to this parameter so long as it falls between 1.0 and 1.5. In following an equivalent procedure for minimizing the Von Mises buckling pressure, Windenburg and Trilling¹⁰ obtained the value 1.265.

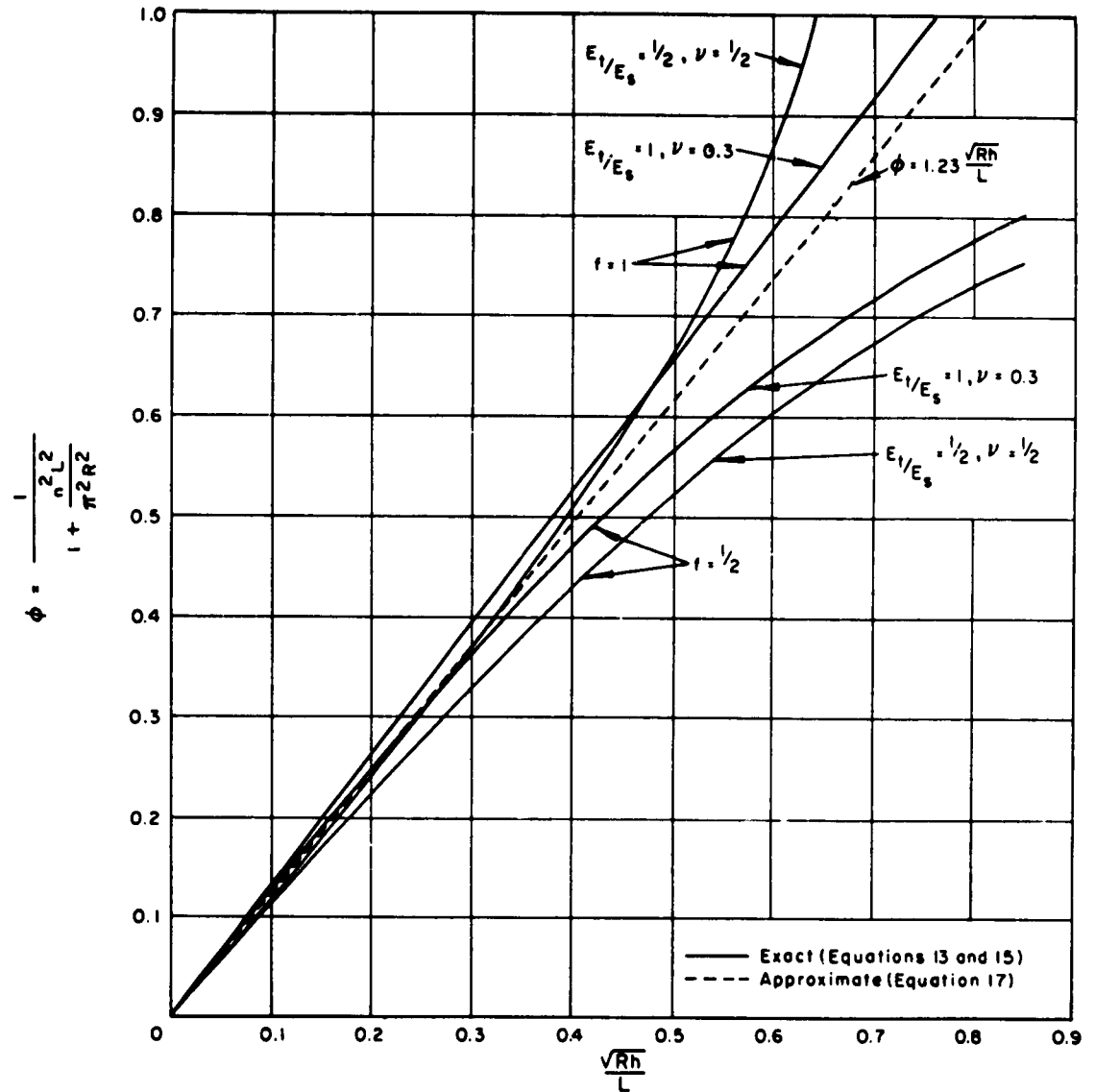


Figure 1 – Buckling-Mode Parameter ϕ as a Function of \sqrt{Rh}/L
 ϕ has the limiting value 1 corresponding to $n = 0$ which defines axisymmetric buckling.

simplifies Equation [14] for the plastic buckling pressure. That equation can be rearranged so that

$$p_p = \frac{8\pi^2 E_t f_p}{9} \left(\frac{h}{R} \right)^2 \left(\frac{\sqrt{Rh}}{L} \right)^2 \left[\frac{1 + \frac{3C\phi}{4}}{3 - 2\phi(1-f_p)} \right] \frac{(1-a)}{\phi} \quad [18]$$

where

$$a = \frac{C\phi^3(1-f_p)}{2 \left[3 - 2\phi(1-f_p) + \frac{3C\phi^2}{4} \right]} \quad [19]$$

The subscript on ϕ_p has been dropped, since the single function ϕ is to be used in both the elastic and plastic regions. It can be seen that a will take on its maximum value when ϕ is equal to 1. For the case $E_t/E_s = 1/2$, a is 0.091 when f_p is $1/2$, and 0 when f_p is 1. Thus for all cases where $E_t/E_s \geq 1/2$, $0 \leq a \leq 0.091$. Since E_t/E_s will seldom be much smaller than $1/2$ whereas ϕ will always be less than 1, the approximation that a can be neglected will introduce only small errors. Equation [18] is thus reduced to

$$p_p = \frac{8\pi^2 E_t f_p}{9\phi} \left(\frac{h}{R} \right)^2 \left(\frac{\sqrt{R}h}{L} \right)^2 \left[\frac{1 + \frac{3C\phi}{4}}{3 - 2\phi(1-f_p)} \right] \quad [20]$$

To examine the accuracy of the equations thus obtained, the results of the approximate equations are compared with those of the exact equations in Figure 2, where $\frac{p}{E_t} \left(\frac{R}{h} \right)^2$ is plotted as a function of $\sqrt{R}h/L$, p being the theoretical buckling pressure. The solid curves represent the exact Equations [14] and [16] for the plastic and elastic cases, respectively, with the corresponding values of ϕ determined from the exact curves of Figure 1. The corresponding approximate results, indicated in Figure 2 by the dotted curves, are obtained from Equations [20] and [16] using the approximate expression [17] for ϕ . It is seen that the approximate method of calculation agrees quite closely with the exact method, even though Figure 1 shows wide divergence between the approximate and exact values for ϕ , particularly in the upper range of $\sqrt{R}h/L$.

DETERMINATION OF SECANT AND TANGENT MODULI

Before Equation [20] can be used, E_s and E_t must be related to the applied pressure. The secant and tangent moduli

$$E_s = \frac{\sigma_i}{\epsilon_i} \quad [21]$$

$$E_t = \frac{d\sigma_i}{d\epsilon_i}$$

are defined in the Appendix and are shown graphically in Figure 3. For hydrostatic pressure

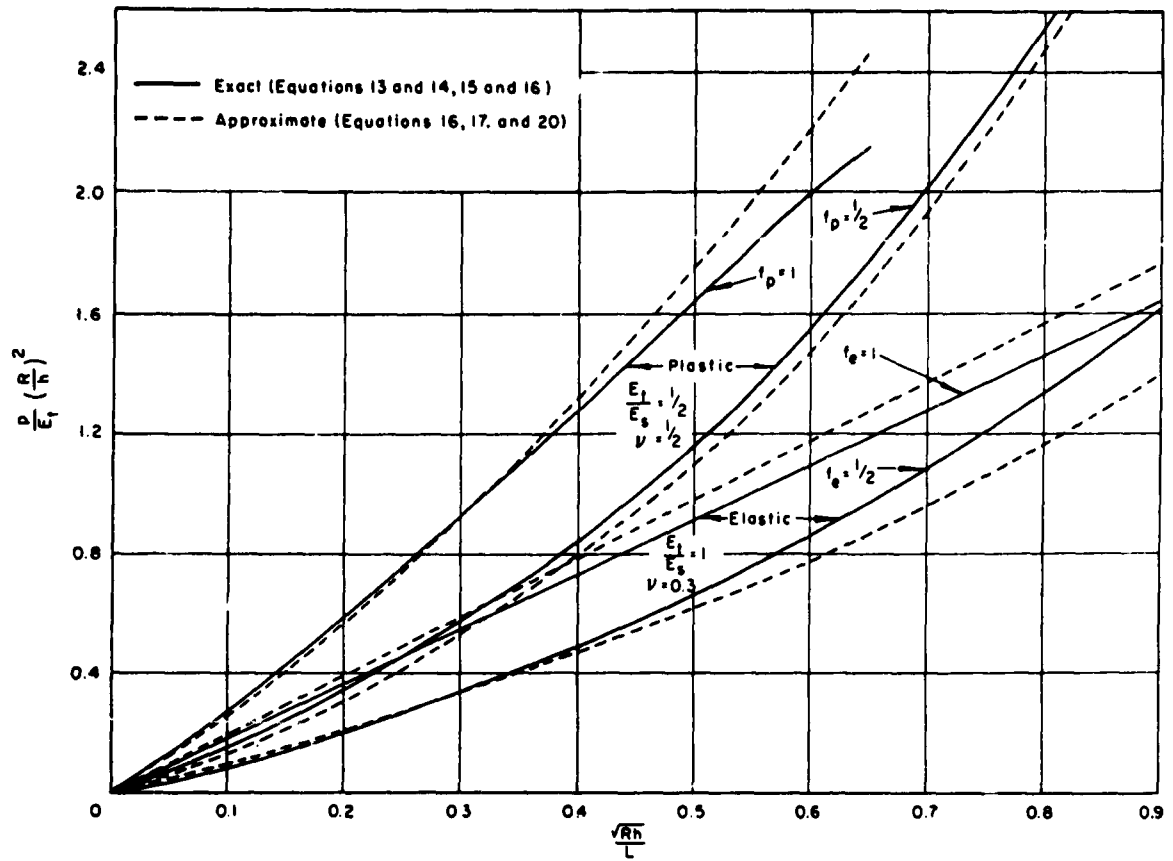


Figure 2 – Comparison of Approximate and Exact Methods for Determining Minimum Buckling Pressure

loading, and with Poisson's ratio equal to $\frac{1}{2}$, the stress and strain intensities are

$$\sigma_i = (\sigma_x^2 + \sigma_s^2 - \sigma_x \sigma_s)^{1/2}$$

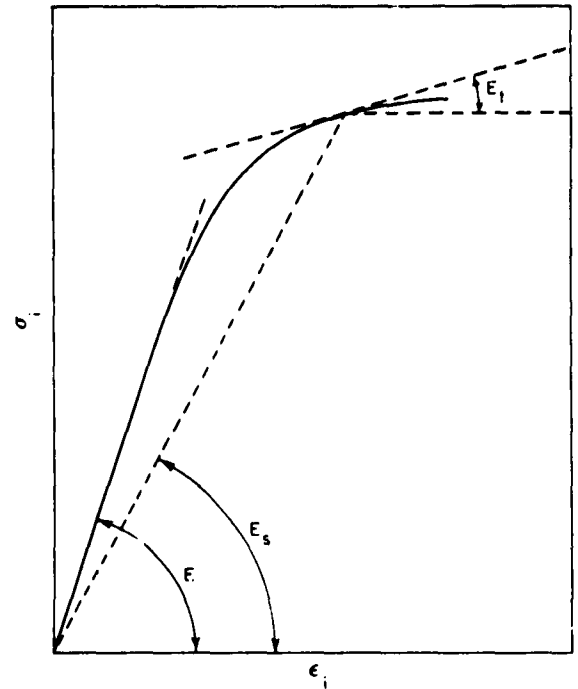
[22]

$$\epsilon_i = \frac{2}{\sqrt{3}} (\epsilon_x^2 + \epsilon_s^2 + \epsilon_x \epsilon_s)^{1/2}$$

The characteristic stress-strain curve of the shell material is first obtained from uniaxial compression tests. In this case σ_i and ϵ_i are identical with the axial stress and strain (regardless of the value of Poisson's ratio). Hence E_s and E_t are readily determined from the stress-strain curve. In practice, it is convenient to determine E_t by drawing tangents to the curve.

Mention should be made of one difficulty which may be encountered in the interpretation of the stress-strain data. Conventional strain-measuring equipment such as an automatic recording extensometer, although adequate for measuring yield strength, may not be sufficiently accurate for the determination of Young's modulus. Unless a high-precision device

Figure 3 – Typical Stress-Strain Diagram



is employed, it is best to obtain only the relative values E_s/E and E_t/E from the stress-strain data and assume a standard value for E .

Having determined E_s/E and E_t/E as functions of σ_i , one must then apply them to the hydrostatically loaded cylindrical shell. According to a fundamental hypothesis of plasticity theory, the stress and strain intensities are uniquely defined.⁴ Thus by expressing hydrostatic pressure in terms of the stress intensity, a relationship between E_s , E_t , and pressure will be established. Since equilibrium requires that σ_x be equal to $pR/2h$, only σ_s in Equation [20] remains to be determined. As discussed in the Appendix, σ_s is actually a continuously varying function of x , whereas in this theory σ_s is treated as a constant. Thus a single value of σ_s must be chosen, and it is taken to be the stress occurring midway between frames. Since this is, generally, the maximum membrane stress in the shell, it might be regarded as a conservative choice. However, it should be noted that for a material exhibiting a plateau-type stress-strain curve, any other choice would probably overestimate the strength of the shell.

In calculating σ_s it is particularly useful to make the further simplifying assumption that σ_s is proportional to the applied pressure in both the elastic and plastic regions. This assumption is reasonable provided the deflections of the shell remain small compared with its thickness. Then σ_s can be determined completely from the theory of Von Sanden and Gunther⁹ with ν equal to $1/2$:

$$\sigma_s = \frac{pR}{h} \left[1 - \frac{0.75 \frac{A_f}{Lh} \left(\beta_p' - \frac{1}{2} \beta_p \right)}{\frac{1}{2} \beta_p \left(\frac{A_f + bh}{Lh} \right) + 1} \right] \quad [23]$$

where

$$\begin{aligned} \beta_p &= \theta_p \left(\frac{\sinh \theta_p + \sin \theta_p}{\cosh \theta_p - \cos \theta_p} \right) \\ \beta_p' &= \frac{\theta_p}{2} \left(\frac{\sinh \frac{\theta_p}{2} + \sin \frac{\theta_p}{2}}{\cosh \frac{\theta_p}{2} - \cos \frac{\theta_p}{2}} \right) \\ \theta_p &= (2.25)^{1/4} \frac{L}{\sqrt{Rh}} \end{aligned} \quad [24]$$

A_f is the cross-sectional area of the frame, and b is the faying width of the frame. The subscript p indicates that all functions are given for Poisson's ratio equal to $1/2$.

It will be observed that the "beam-column" effect, demonstrated theoretically by Salerno and Pulos,¹¹ is ignored in the assumption of proportional loading. This effect causes a departure from proportional loading in the elastic region. However, this departure is ordinarily small and, in view of the approximations already made, to account for it would be an unnecessary refinement. In those cases where the effect is large it can easily be included in the value assumed for σ_s .*

The stress ratio for Poisson's ratio equal to $1/2$ is then given by

$$f_p = \frac{0.5}{\left[1 - \frac{0.75 \frac{A_f}{Lh} \left(\beta_p' - \frac{1}{2} \beta_p \right)}{\frac{1}{2} \beta_p \left(\frac{A_f + bh}{Lh} \right) + 1} \right]} \quad [25]$$

*Additional departures from proportional loading are exhibited by cylinders whose generators are not initially straight. This effect can be computed from an analysis by Luncheon and Short.¹²

Solving Equation [22] for the applied pressure, one obtains

$$p = \frac{2\sigma_i h f_p}{R\sqrt{f_p^2 - f_p + 1}} \quad [26]$$

A plot of p versus σ_i from this equation is a straight line for the case of proportional loading but becomes a curve if the aforementioned nonlinear effects are included.

INELASTIC BUCKLING

Although Equations [16], [20], and [26] define the buckling pressure for the elastic and the fully plastic regions, no solution is given for the inelastic region which lies between these two limiting cases. However, by employing an empirical correction factor wherein Poisson's ratio is regarded as a variable, one can arrive at an expression which reduces to the proper limiting values. Gerard and Wildhorn¹³ have found that ν can be accurately expressed as a function of E_s in the inelastic region by the equation

$$\nu = \frac{1}{2} - \frac{E_s}{E} \left(\frac{1}{2} - \nu_e \right) \quad [27]$$

which reduces to $\frac{1}{2}$ when E_s/E is zero and to ν_e when E_s/E is one. Since Equation [20] is for the fully plastic case where ν has the value $\frac{1}{2}$, it could be written

$$p_p = \frac{2\pi^2 E_t f_p}{3\phi \left[1 - \left(\frac{1}{2} \right)^2 \right]} \left(\frac{h}{R} \right)^2 \left(\frac{\sqrt{R}h}{L} \right)^2 \left[\frac{1 + \frac{3C\phi}{4}}{3 - 2\phi(1 - f_p)} \right] \quad [28]$$

If $\frac{1}{2}$ is now replaced by ν , a variable defined by Equation [27] and f_p is replaced by f , a function of ν , the equation for p_c , the buckling pressure in the inelastic region, is

$$p_c = \frac{2\pi^2 E_t f}{3\phi(1 - \nu^2)} \left(\frac{h}{R} \right)^2 \left(\frac{\sqrt{R}h}{L} \right)^2 \left[\frac{1 + \frac{3\phi}{4} \left(\frac{E_s}{E_t} - 1 \right)}{3 - 2\phi(1 - f)} \right] \quad [29]$$

With ϕ given by Equation [17], p_c reduces to p_p when E_s/E is zero and to p_e , given by Equation [16], when E_s/E is one. From Equation [29] it can be seen that the inelastic buckling pressure depends on both the tangent and secant moduli.

In determining the stress ratio f , σ_s is again taken to be the stress midway between frames as given by the theory of Von Sanden and Gunther,⁹ but with ν a variable defined by Equation [27]. It is found, however, that σ_s is practically insensitive to variations in ν and that it is sufficient to treat f as a constant which depends only on the geometry of the cylinder. This is the same as assuming that σ_s is proportional to the applied pressure. Since it has been found in practice that variations in ν are small, ν_e can be used for determining the stress ratio. In this way p_c will still reduce to p_e when E_s/E is equal to one, and Equation [29] can be written

$$p_c = p_e \left(\frac{1 - \nu_e^2}{1 - \nu^2} \right) \left[\frac{E_t}{E} \left(1 - \frac{3\phi}{4} \right) + \frac{3\phi}{4} \frac{E_s}{E} \right] \quad [30]$$

where

$$p_e = \frac{2\pi^2 E f_e}{3\phi(1 - \nu_e^2)} \left(\frac{h}{R} \right)^2 \frac{\left(\frac{\sqrt{Rh}}{L} \right)^2}{3 - 2\phi(1 - f_e)} \quad [16]$$

$$\phi = 1.23 \frac{\sqrt{Rh}}{L} \quad [17]$$

$$f_e = \frac{0.5}{1 - \frac{\left(1 - \frac{\nu_e}{2} \right) \frac{A_f}{Lh} \left(\beta_e' - \frac{1}{2} \beta_e \right)}{\frac{1}{2} \beta_e \left(\frac{A_f + bh}{Lh} \right) + 1} \quad [31]$$

and

$$\begin{aligned} \beta_e &= \theta_e \left(\frac{\sinh \theta_e + \sin \theta_e}{\cosh \theta_e - \cos \theta_e} \right) \\ \beta_e' &= \frac{\theta_e}{2} \left(\frac{\sinh \frac{\theta_e}{2} + \sin \frac{\theta_e}{2}}{\cosh \frac{\theta_e}{2} - \cos \frac{\theta_e}{2}} \right) \\ \theta_e &= [3(1 - \nu_e^2)]^{1/4} \frac{L}{\sqrt{Rh}} \end{aligned} \quad [32]$$

The subscript e designates functions based on the elastic value of Poisson's ratio.

The inelastic buckling pressure p_c can now be determined as follows: from the characteristic stress-strain curve of the shell material, E_s/E and E_t/E are defined in terms of σ_i , the stress intensity. Hence p_c can be plotted as a function of σ_i using Equation [30]. Similarly, the applied pressure p can be plotted against σ_i from Equation [26]. Since Equation [30] is valid only when p_c and p are equal, the buckling pressure is obtained from the intersection of the two plots.

Figure 4 illustrates the two general types of material encountered in practice. The first is the strain-hardening type (Figure 4a) which exhibits a continuous stress-strain curve. Plots of Equations [26] and [30] are shown in Figure 4b, where the buckling pressure is defined by the intersection of the two curves. Figure 4c illustrates the case of an elastic-perfectly-plastic material. Since the buckling pressure abruptly drops to zero when the plastic region is reached, collapse is simply defined at the elastic limit of the material, as shown in Figure 4d.

EVALUATION OF THEORY WITH EXPERIMENTAL DATA ON STIFFENED CYLINDERS

To evaluate the theory, results were examined from previous tests of seven cylinders in which asymmetric (lobar) shell failures were observed. The properties of these cylinders, all of which had external stiffeners, are listed in Table 1. Two were machined from seamless steel tubing and had rectangular stiffeners. The other five had T-stiffeners and were rolled and welded from U.S. Steel Carilloy steel plate. As indicated by the symbol (c) in Table 1, in some cases specimens were taken from the collapsed cylinder, whereas in others (unmarked) they were taken prior to fabrication. Data from uniaxial compression tests of these specimens were used for the measurement of yield strength and for the determination of the secant and tangent moduli. Since all data were obtained with an automatic recording extensometer, which was not sufficiently precise for the absolute determination of Young's modulus, only the relative values E_s/E and E_t/E were determined from these data. For all cylinders a standard value of 30×10^6 psi was used as Young's modulus E . Plots of σ_i versus ϵ_i for the seven cylinders are shown in Figure 5.

In Table 2 the experimental collapse pressures are compared with the inelastic buckling pressures calculated from the theory of this report (Equation [30]). This information is also presented graphically in Figure 6, where the ratio of theoretical pressure to the elastic buckling pressure p_e (Equation [16]) is plotted against the ratio of experimental pressure to p_e .

Table 2 also lists failure pressures predicted by several other criteria. Elastic buckling pressures were calculated from Equation [16] of this report, from the theory of Von Sanden and Tölké,⁸ and from the theory of Von Mises using the approximate EMB formula [10].¹⁰ Shell failure pressures are given for Von Sanden and Gunther formula [92a]⁹ (based on simple yielding of the exterior shell fiber at midbay) and for the Hencky-Von Mises criterion applied

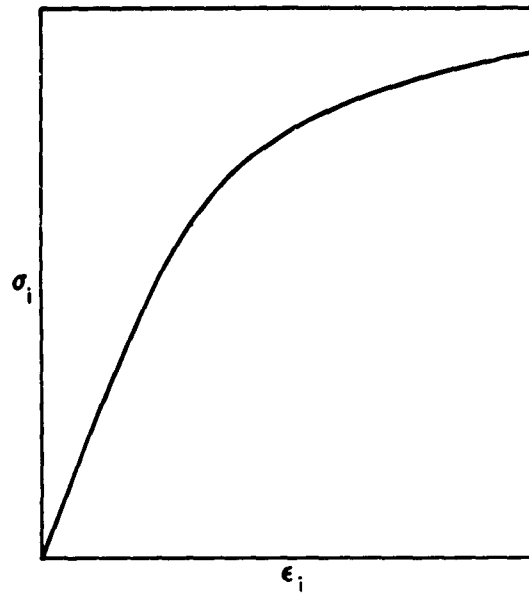


Figure 4a

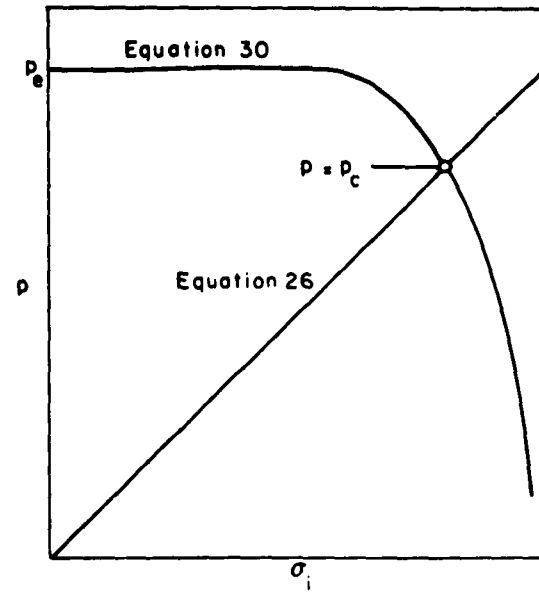


Figure 4b

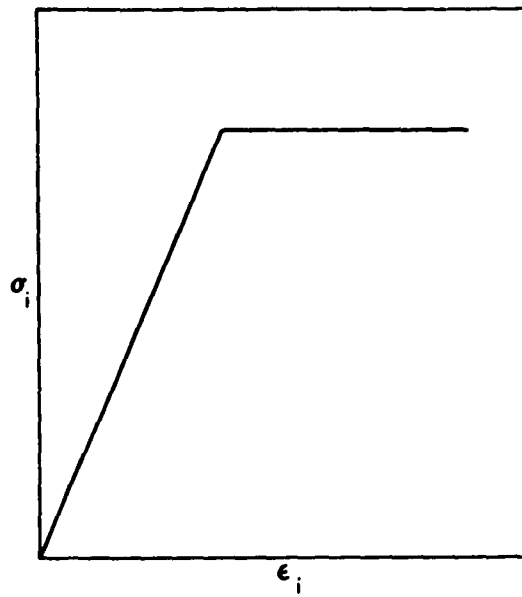


Figure 4c

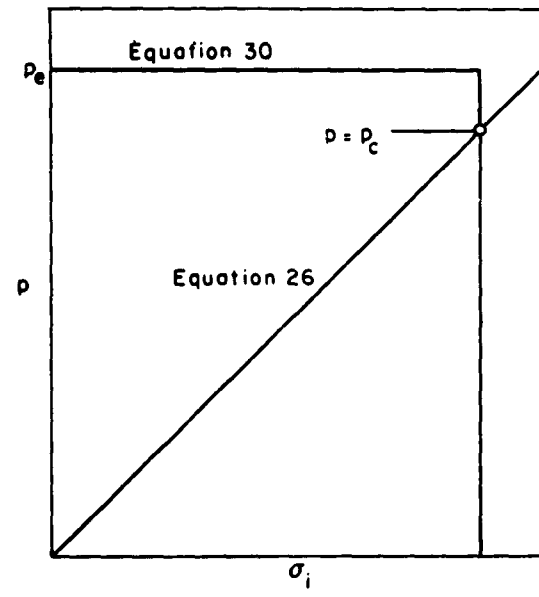


Figure 4d

Figure 4 – Graphical Determination of Buckling Pressure for Two General Classes of Material

TABLE 1
Properties of Cylinders

Cylinder		Radius R in.	Shell Thickness h in.	Unsupported Length of Shell L in.	Frame Area A_f sq in.	Frame Faying Width b in.	Yield Strength σ_y^* psi
Welded with T-Frames	T- 2	38.87	0.264	7.24	1.885	0.260	88,000 (c)
	T- 3	38.87	0.260	8.74	1.625	0.260	108,000 (c)
	T- 6	26.87	0.256	7.24	1.170	0.260	115,000 (c)
	T- 2A	38.87	0.254	7.24	0.796	0.260	103,000
	T- 7A	26.87	0.263	8.74	0.683	0.260	84,000
Machined with Rectangular Frames	U-12	4.081	0.0446	1.06	0.0248	0.079	68,000
	U-22	4.077	0.0356	0.834	0.0185	0.068	70,500
<p>*All yield strengths are defined at offset strain of 0.002.</p> <p>(c) Specimens of shell material taken from collapsed cylinder. Specimens for all other cylinders were obtained prior to fabrication.</p>							

TABLE 2
Comparison of Theoretical and Experimental Collapse Pressures

Cylinder Number		Welded					Machined	
		T-2	T-3	T-6	T-2A	T-7A	U-12	U-22
Experimental Collapse Pressure		670	553	1005	680	770	975	735
Inelastic Buckling	Equation [30] (p_c)	696	563	1016	705	748	938	734
Elastic Buckling	Von Sanden and Tölke ⁸	930	631	1258	773	1032	2014	1054
	Equation [16] (p_e)	906	626	1259	756	1010	1907	1002
	Von Mises ¹⁰ (EMB Formula [10])	786	585	1180	705	995	1786	963
Shell Yield	Hencky-Von Mises midbay, midplane	903	953	1429	912	976	1081	777
	Von Sanden and Gunther Formula [92A] ⁹	695	742	1121	733	799	788	622

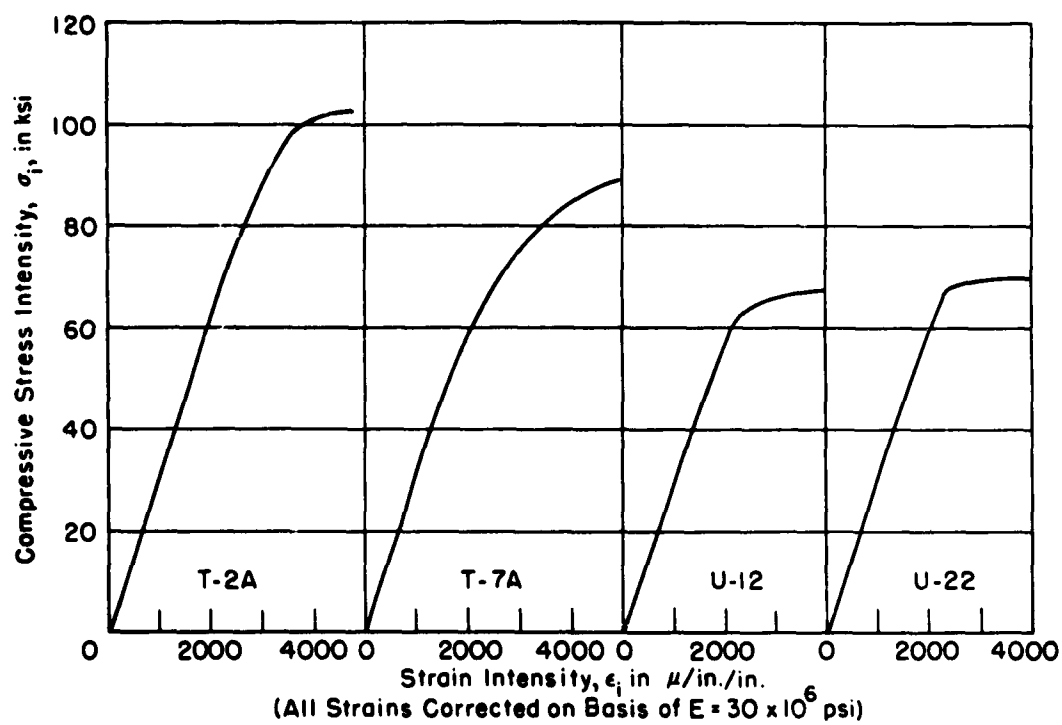
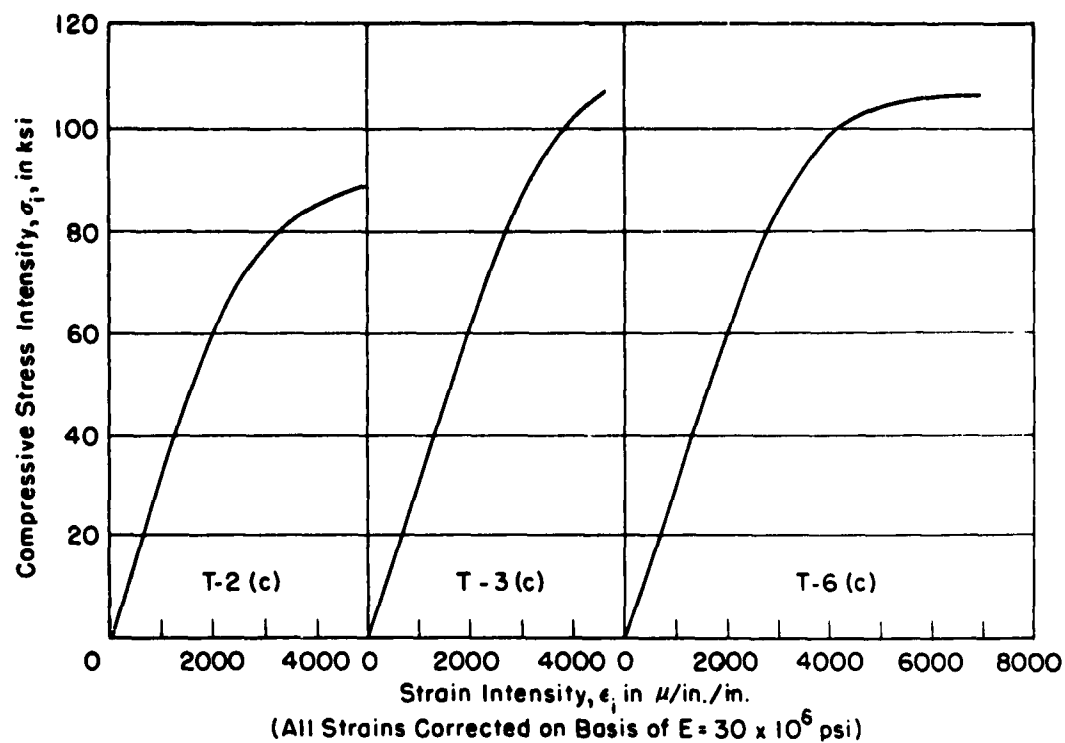


Figure 5 - Compression Curves for Cylinder Materials

(c) Material taken from collapsed cylinder

Axis of load corresponds to circumferential direction in cylinder

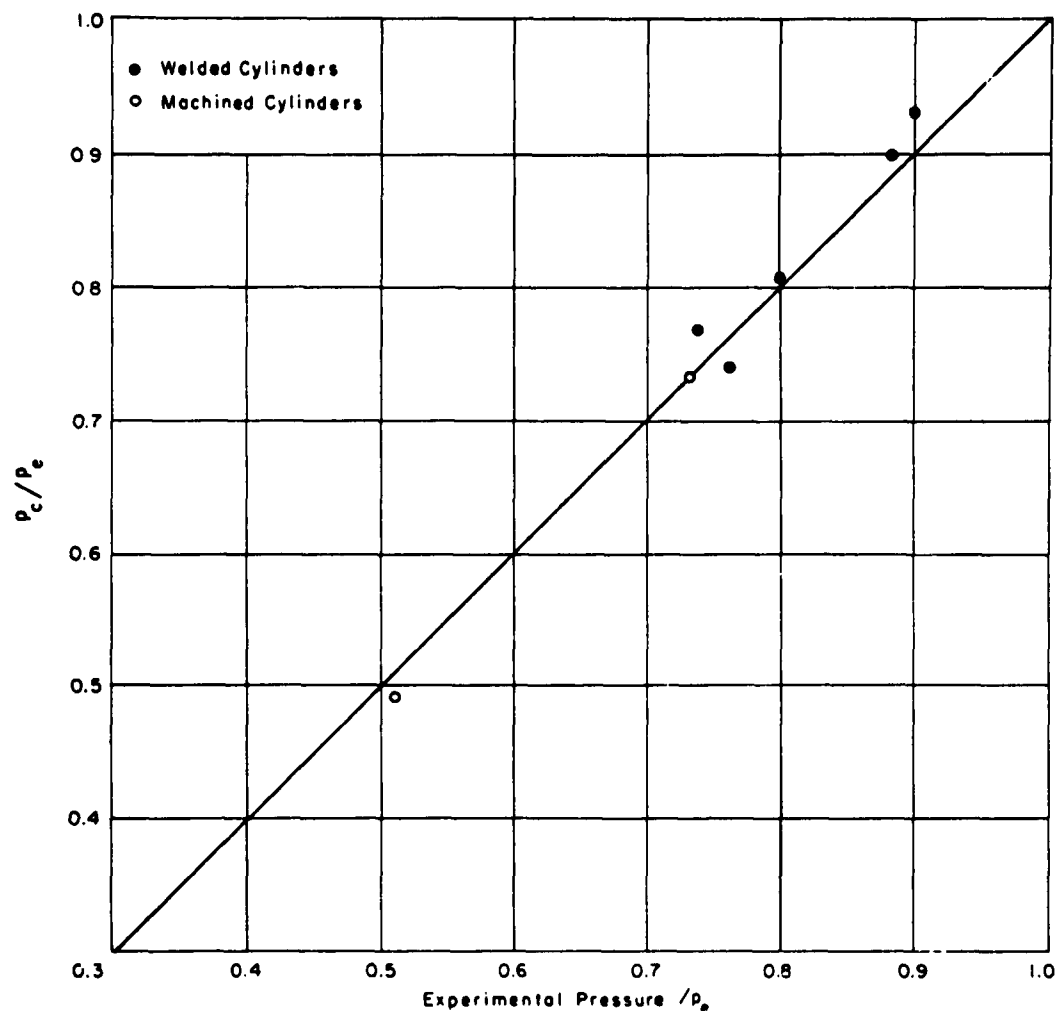


Figure 6 – Comparison of Theoretical and Experimental Collapse Pressures

p_c = Inelastic Buckling Pressure (Equation [30])

p_e = Elastic Buckling Pressure (Equation [16])

to the membrane stress at midbay, wherein failure is assumed to occur when the stress intensity, σ_i , computed from the theory of Von Sander and Gunther, reaches the yield strength of the shell material.

From Table 2 and Figure 6, it can be seen that Equation [30] is in close agreement (within 4 percent) for all cylinders reported. In view of the many approximations contained in the theory, this agreement is considered surprisingly good. It is also noted that for all welded cylinders except T-7A the pressures according to Equation [30] are higher than those observed. This is to be expected, since such cylinders are weakened by residual stresses and geometrical imperfections introduced during fabrication, none of which are accounted for in the theory. However, good correlation in these cases indicates that such weakening

effects may not be as severe as had previously been suspected. From the uniformity of the results there also appears to be no significant difference for the limited available test results between those cases where test specimens were taken before fabrication and those where they were taken from the collapsed cylinder.

CONCLUSIONS

1. The theory of this report, on the basis of the limited test data available, appears to predict the inelastic (lobal) buckling pressure with good accuracy.
2. Final evaluation of the theory must await additional experimental data, which should include tests of cylinders with internal frames.

ACKNOWLEDGMENTS

This work was initiated at the suggestion of Mr. John G. Pulos and has proceeded under his general guidance. The author is greatly indebted to Dr. Myron E. Lunchick, who provided valuable suggestions and advice. Thanks are also due Mr. John E. Buhl, who supplied the experimental data, and to Mr. Abner R. Willner, from whom the stress-strain measurements were obtained.

APPENDIX

DERIVATION OF BUCKLING EQUATIONS

In deriving general plasticity equations for cylinders, Gerard⁵ defines stress and strain intensities for Poisson's ratio equal to $\frac{1}{2}$ according to the octahedral shear law:

$$\sigma_i = (\sigma_x^2 + \sigma_s^2 - \sigma_x \sigma_s + 3\tau^2)^{1/2} \quad [33]$$

$$\epsilon_i = \frac{2}{\sqrt{3}} \left(\epsilon_x^2 + \epsilon_s^2 + \epsilon_x \epsilon_s + \frac{\gamma^2}{4} \right)^{1/2}$$

The secant and tangent moduli are then defined as

$$E_s = \frac{\sigma_i}{\epsilon_i} \quad [34]$$

$$E_t = \frac{d\sigma_i}{d\epsilon_i}$$

With the assumption that Poisson's ratio ν is equal to $\frac{1}{2}$ in both the elastic and plastic region, the stress-strain relations become

$$\epsilon_x = \frac{1}{E_s} \left(\sigma_x - \frac{\sigma_s}{2} \right)$$

$$\epsilon_s = \frac{1}{E_s} \left(\sigma_s - \frac{\sigma_x}{2} \right) \quad [35]$$

$$\gamma = \frac{3\tau}{E_s}$$

The subscript s replaces y in Gerard's notation and refers to the tangential direction, as shown in Figure 7.

In treating the general case, Gerard considers a cylinder subjected to external loads N_x , N_s , and N_{xs} per unit width and external pressure p . The general differential equations of equilibrium are:

$$A_1 \frac{\partial^2 u}{\partial x^2} - \frac{A_{13}}{2} \frac{\partial^2 u}{\partial x \partial s} + \frac{A_3}{4} \frac{\partial^2 u}{\partial s^2} - \frac{A_{13}}{4} \frac{\partial^2 v}{\partial x^2} + \left(\frac{A_{12}}{2} + \frac{A_3}{4} \right) \frac{\partial^2 v}{\partial x \partial s} - \frac{A_{23}}{4} \frac{\partial^2 v}{\partial s^2} + \frac{A_{12}}{2R} \frac{\partial w}{\partial x} - \frac{A_{23}}{4R} \frac{\partial w}{\partial s} = 0$$

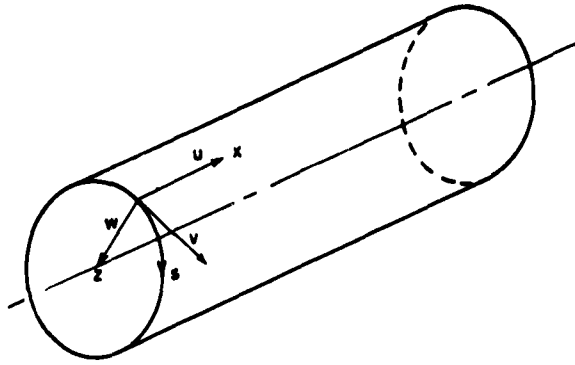
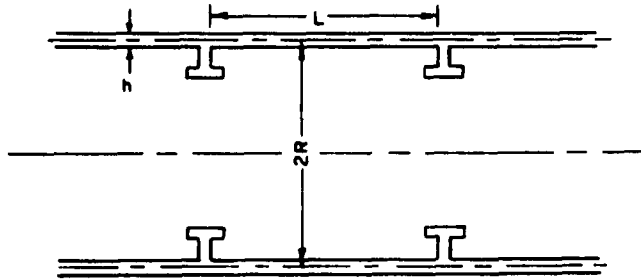


Figure 7 - Coordinate System and Cross Section of Stiffened Shell



$$A_2 \frac{\partial^2 v}{\partial s^2} - \frac{A_{23}}{2} \frac{\partial^2 v}{\partial x \partial s} + \frac{A_3}{4} \frac{\partial^2 v}{\partial x^2} - \frac{A_{13}}{4} \frac{\partial^2 u}{\partial x^2} + \left(\frac{A_{12}}{2} + \frac{A_3}{4} \right) \frac{\partial^2 u}{\partial x \partial s} - \frac{A_{23}}{4} \frac{\partial^2 u}{\partial s^2} + \frac{A_2}{R} \frac{\partial w}{\partial s} - \frac{A_{23}}{4R} \frac{\partial w}{\partial x} = 0 \quad [36]$$

$$D \left[A_1 \frac{\partial^4 w}{\partial x^4} - A_{13} \frac{\partial^4 w}{\partial x^3 \partial s} + (A_{12} + A_3) \frac{\partial^4 w}{\partial x^2 \partial s^2} - A_{23} \frac{\partial^4 w}{\partial x \partial s^3} + A_2 \frac{\partial^4 w}{\partial s^4} \right] + \frac{4E_s h}{3R} \left(\frac{A_{12}}{2} \frac{\partial u}{\partial x} - \frac{A_{23}}{4} \frac{\partial u}{\partial s} - \frac{A_{23}}{4} \frac{\partial v}{\partial x} + \frac{A_2 \partial v}{\partial s} + \frac{A_2 w}{R} \right) + N_x \frac{\partial^2 w}{\partial x^2} + 2N_{xs} \frac{\partial^2 w}{\partial x \partial s} + N_s \frac{\partial^2 w}{\partial s^2} + p = 0$$

In this analysis, long cylinders which buckle in the oval ($n = 2$) mode will be excluded from consideration, since the differential equations are derived with certain approximations which are valid only when $\pi^2 \gg 1$.

The bending rigidity for ν equal to $\frac{1}{2}$ is

$$D = \frac{E_s h^3}{9} \quad [37]$$

Gerard defines the plasticity coefficients as follows:

$$\begin{aligned} A_1 &= 1 - \frac{\alpha \sigma_x^2}{4} \\ A_2 &= 1 - \frac{\alpha \sigma_s^2}{4} \\ A_3 &= 1 - \alpha \tau^2 \\ A_{21} &= A_{12} = 1 - \frac{\alpha \sigma_x \sigma_s}{2} \\ A_{31} &= A_{13} = \alpha \sigma_x \tau \\ A_{32} &= A_{23} = \alpha \sigma_s \tau \end{aligned} \quad [38]$$

where

$$\alpha = \frac{3}{\sigma_i^2} \left(1 - \frac{E_t}{E_s} \right) \quad [39]$$

In the case of uniform hydrostatic pressure, it is readily seen that

$$\begin{aligned} \tau &= \frac{N_{xs}}{h} = 0 \\ \sigma_x &= \frac{N_x}{h} = \frac{pR}{2h} \end{aligned} \quad [40]$$

On the other hand, σ_s is not so easily disposed of. In deriving his equations, Gerard considers N_s as independent of x , an assumption which is correct in the two cases (axial compression and torsion) for which he obtained solutions, but one which is clearly not correct in the case of hydrostatic pressure if the ends of the cylinder are restrained. However, without such an assumption it would be difficult, if not impossible, to solve the problem by means of differential equations. Furthermore, in order to simplify the plasticity coefficients, the additional assumption is made that

$$\sigma_s = \frac{N_s}{h} = \frac{pR}{h} \quad [41]$$

whereby the stress intensity becomes

$$\sigma_t = \sigma_x \sqrt{3} \quad [42]$$

and the resulting plasticity coefficients are

$$\begin{aligned} A_1 &= \frac{3}{4} + \frac{E_t}{4E_s} \\ A_2 &= A_{21} = A_{12} = \frac{E_t}{E_s} \\ A_3 &= 1 \\ A_{13} &= A_{31} = A_{23} = A_{32} = 0 \end{aligned} \quad [43]$$

Although it would logically follow that N_s in Equation [36] should be replaced by pR , this substitution is not necessary for the solution of the differential equations. Instead, by retaining N_s as an arbitrary factor, a more general solution can be obtained. The load N_s can later be determined from appropriate theory, as described in the body of this report. The resulting differential equations are:

$$\frac{E_t}{2E_s} \left(\frac{1}{2} \frac{\partial^2 u}{\partial x^2} + \frac{\partial^2 v}{\partial x \partial s} + \frac{1}{R} \frac{\partial w}{\partial x} \right) + \frac{3}{4} \frac{\partial^2 u}{\partial x^2} + \frac{1}{4} \frac{\partial^2 u}{\partial s^2} + \frac{1}{4} \frac{\partial^2 v}{\partial x \partial s} = 0 \quad [1a]$$

$$\frac{E_t}{E_s} \left(\frac{1}{2} \frac{\partial^2 u}{\partial x \partial s} + \frac{\partial^2 v}{\partial s^2} + \frac{1}{R} \frac{\partial w}{\partial s} \right) + \frac{1}{4} \frac{\partial^2 v}{\partial x^2} + \frac{1}{4} \frac{\partial^2 u}{\partial x \partial s} = 0 \quad [1b]$$

$$\begin{aligned} \frac{4E_s h}{3R} \left(\frac{E_t}{E_s} \right) \left(\frac{1}{2} \frac{\partial u}{\partial x} + \frac{\partial v}{\partial s} + \frac{w}{R} \right) + D \left[\frac{E_t}{E_s} \left(\frac{1}{4} \frac{\partial^4 w}{\partial x^4} + \frac{\partial^4 w}{\partial x^2 \partial s^2} \right. \right. \\ \left. \left. + \frac{\partial^4 w}{\partial s^4} \right) + \frac{3}{4} \frac{\partial^4 w}{\partial x^4} + \frac{\partial^4 w}{\partial x^2 \partial s^2} \right] + N_s \frac{\partial^2 w}{\partial x^2} \\ + N_s \frac{\partial^2 w}{\partial s^2} + p = 0 \end{aligned} \quad [1c]$$

REFERENCES

1. Bijlaard, P.P., "Theory and Tests on the Plastic Stability of Plates and Shells," *Journal Aeronautical Science*, Vol. 16, No. 9 (Sep 1949).
2. Bijlaard, P.P., "On the Plastic Stability of Thin Plates and Shells," *Verh. Koninklijke Nederlandsche Akademie van Wetenschappen*, Vol. L, No. 7 (Sep 1947).
3. Ilyushin, A.A., "The Elasto-plastic Stability of Plates," *National Advisory Committee for Aeronautics*, Technical Memorandum 1188 (Dec 1947).
4. Stowell, E.Z., "A Unified Theory of Plastic Buckling of Columns and Plates," *National Advisory Committee for Aeronautics Report* 898 (1948).
5. Gerard, G., "Compressive and Torsional Buckling of Thin-wall Cylinders in Yield Region," *National Advisory Committee for Aeronautics Technical Note* 3726 (Aug 1956).
6. Lunchick, M.E., "Plastic Axisymmetric Buckling of Ring-Stiffened Cylindrical Shells Fabricated from Strain-Hardening Materials and Subjected to External Hydrostatic Pressure," *David Taylor Model Basin Report* to be published.
7. Donnell, L.H., "Stability of Thin-walled Tubes under Torsion," *National Advisory Committee for Aeronautics Technical Report* 479 (1933).
8. Von Sanden, K. and Tölke, F., "On Stability Problems in Thin Cylindrical Shells" (*über Stabilitätsprobleme Dünner, Kreiszyklindrischer Schalen*), *Ingenieur-Archiv*, Vol. 3, pp. 24-66 (1932), *David Taylor Model Basin Translation* 33 (Dec 1949).
9. Von Sanden, K. and Gunther, K., "The Strength of Cylindrical Shells, Stiffened by Frames and Bulkheads, under Uniform External Pressure on All Sides," (*Über das Festigkeitsproblem guerversteifter Hohlzylinder unter allseitig gleichmässigem Aussendruck*), *Werft-Reederei-Hafen*, Vol. 1 (1920), Nos. 8, 9, and 10, and Vol. 2 (1921), No. 17. See *David Taylor Model Basin Translation* 38 (Mar 1952).
10. Windenburg, D.F. and Trilling, C., "Collapse by Instability of Thin Cylindrical Shells under External Pressure," *Transactions, American Society of Mechanical Engineers*, Vol. 56, No. 11 (1934). Also *Experimental Model Basin Report* 385 (Jul 1934).
11. Salerno, V.L. and Pulos, J.G., "Stress Distribution in a Circular Cylindrical Shell under Hydrostatic Pressure Supported by Equally Spaced Circular Ring Frames," *Polytechnic Institute of Brooklyn, Department of Aeronautical Engineering and Applied Mechanics*, Report 171-A (Jun 1951).
12. Lunchick, M.E. and Short, R.D., Jr., "Behavior of Cylinders with Initial Shell Deflection," *Journal of Applied Mechanics*, Vol. 24, No. 4, pp. 559-564 (Dec 1957).
13. Gerard, G. and Wildhorn, S., "A Study Of Poisson's Ratio in the Yield Region," *National Advisory Committee for Aeronautics Technical Note* 2561 (Jun 1952).

INITIAL DISTRIBUTION

Copies

- 13 CHBUSHIPS
 - 3 Tech Info Br (Code 335)
 - 1 Tech Asst (Code 106)
 - 1 Prelim Des Br (Code 420)
 - 1 Prelim Des Sec (Code 421)
 - 1 Ship Protec (Code 423)
 - 1 Hull Des Br (Code 440)
 - 2 Sci and Res Sec (Code 442)
 - 1 Struc Sec (Code 443)
 - 1 Submarine Br (Code 525)
 - 1 Hull Arr, Struc and Preserv Br (Code 633)
- 2 CHONR
 - Struc Mech (Code 439)
- 2 CNO
 - Res and Dev Div, Undersea Warfare Sec (Op 702C)
- 1 CDR, USNOL
- 1 CO, USNROTC and USNAVADMINU MIT
- 1 DIR, USNRL, Attn: TID (Code 2027)
- 1 DIR of DEF R and E, Attn: Tech Library
- 2 NAVSHIPYD MARE
- 1 NAVSHIPYD NORVA, Attn: UERD (Code 280)
- 2 NAVSHIPYD PTSMH
- 1 SUPSHIP, Groton
- 1 SUPSHIP, Newport News
- 1 SUPSHIP, Pascagoula
- 1 NNS & DD CO
- 1 Ingalls Shipbldg Corp
- 1 Elec Boat Div, Genl Dyn Corp
- 1 O in C, PGSCOL, Webb
- 1 G. Gerard, College of Engin, New York Univ, New York

David Taylor Model Basin. Report 1392.

INELASTIC LOBAR BUCKLING OF CYLINDRICAL SHELLS UNDER EXTERNAL HYDROSTATIC PRESSURE, by Thomas E. Reynolds. Aug 1960. iv, 27p. illus., tables, refs. UNCLASSIFIED

A solution to Gerard's differential equations for plastic buckling of cylindrical shells is found for the case of lobar buckling under hydrostatic pressure. An approximate formula based on this solution is then obtained for buckling in the inelastic region.

According to this formula, the buckling pressure is a function of the cylinder geometry and the secant and tangent moduli as determined from a stress-strain intensity diagram for the shell material. Agreement with experiments on ring-stiffened cylinders is found to be within 4 percent.

1. Cylindrical shells (Stiffened) - Buckling - Mathematical analysis
2. Cylindrical shells (Stiffened) - Buckling - Theory

I. Reynolds, Thomas E.
II. S-F013 03 02

David Taylor Model Basin. Report 1392.

INELASTIC LOBAR BUCKLING OF CYLINDRICAL SHELLS UNDER EXTERNAL HYDROSTATIC PRESSURE, by Thomas E. Reynolds. Aug 1960. iv, 27p. illus., tables, refs. UNCLASSIFIED

A solution to Gerard's differential equations for plastic buckling of cylindrical shells is found for the case of lobar buckling under hydrostatic pressure. An approximate formula based on this solution is then obtained for buckling in the inelastic region.

According to this formula, the buckling pressure is a function of the cylinder geometry and the secant and tangent moduli as determined from a stress-strain intensity diagram for the shell material. Agreement with experiments on ring-stiffened cylinders is found to be within 4 percent.

1. Cylindrical shells (Stiffened) - Buckling - Mathematical analysis
 2. Cylindrical shells (Stiffened) - Buckling - Theory
- I. Reynolds, Thomas E.
II. S-F013 03 02

David Taylor Model Basin. Report 1392.

INELASTIC LOBAR BUCKLING OF CYLINDRICAL SHELLS UNDER EXTERNAL HYDROSTATIC PRESSURE, by Thomas E. Reynolds. Aug 1960. iv, 27p. illus., tables, refs. UNCLASSIFIED

A solution to Gerard's differential equations for plastic buckling of cylindrical shells is found for the case of lobar buckling under hydrostatic pressure. An approximate formula based on this solution is then obtained for buckling in the inelastic region.

According to this formula, the buckling pressure is a function of the cylinder geometry and the secant and tangent moduli as determined from a stress-strain intensity diagram for the shell material. Agreement with experiments on ring-stiffened cylinders is found to be within 4 percent.

1. Cylindrical shells (Stiffened) - Buckling - Mathematical analysis
2. Cylindrical shells (Stiffened) - Buckling - Theory

I. Reynolds, Thomas E.
II. S-F013 03 02

David Taylor Model Basin. Report 1392.

INELASTIC LOBAR BUCKLING OF CYLINDRICAL SHELLS UNDER EXTERNAL HYDROSTATIC PRESSURE, by Thomas E. Reynolds. Aug 1960. iv, 27p. illus., tables, refs. UNCLASSIFIED

A solution to Gerard's differential equations for plastic buckling of cylindrical shells is found for the case of lobar buckling under hydrostatic pressure. An approximate formula based on this solution is then obtained for buckling in the inelastic region.

According to this formula, the buckling pressure is a function of the cylinder geometry and the secant and tangent moduli as determined from a stress-strain intensity diagram for the shell material. Agreement with experiments on ring-stiffened cylinders is found to be within 4 percent.

1. Cylindrical shells (Stiffened) - Buckling - Mathematical analysis
 2. Cylindrical shells (Stiffened) - Buckling - Theory
- I. Reynolds, Thomas E.
II. S-F013 03 02